



Published in final edited form as:

*Mol Cancer Ther.* 2017 November ; 16(11): 2399–2409. doi:10.1158/1535-7163.MCT-16-0452.

## Dual inhibition of Hedgehog and c-Met pathways for pancreatic cancer treatment

Agnieszka A. Rucki<sup>1,2,3,\*</sup>, Qian Xiao<sup>4,5,1,2,\*</sup>, Stephen Muth<sup>1,2</sup>, Jianlin Chen<sup>1,2,6</sup>, Xu Che<sup>1,2</sup>, Jennifer Kleponis<sup>1,2</sup>, Rajni Sharma<sup>8</sup>, Robert A. Anders<sup>1,2,8</sup>, Elizabeth M. Jaffee<sup>1,2,3,8,10</sup>, and Lei Zheng<sup>1,2,3,9,10</sup>

<sup>1</sup>The Sidney Kimmel Comprehensive Cancer Center, the Second Affiliated Hospital of the Zhejiang University School of Medicine, Hangzhou, China 310009

<sup>2</sup>Department of Oncology, the Second Affiliated Hospital of the Zhejiang University School of Medicine, Hangzhou, China 310009

<sup>3</sup>Graduate Program in Cellular and Molecular Medicine, the Second Affiliated Hospital of the Zhejiang University School of Medicine, Hangzhou, China 310009

<sup>4</sup>Department of Surgical Oncology, the Second Affiliated Hospital of the Zhejiang University School of Medicine, Hangzhou, China 310009

<sup>5</sup>Zhejiang University School of Medicine, Hangzhou, China 310009

<sup>6</sup>Department of Hepatobiliary Oncology, Sun Yat-sen University Cancer Center, State Key Laboratory of Southern China, Collaborative Innovation Center for Cancer Medicine, Guangzhou 510060, China

<sup>7</sup>Pancreatic and gastric surgery department, Cancer hospital, Peking Union medical college, Chinese academy of medical sciences 100021

<sup>8</sup>Department of Pathology, The Johns Hopkins University School of Medicine, Baltimore, Maryland, 21287, USA

<sup>9</sup>Department of Surgery, The Johns Hopkins University School of Medicine, Baltimore, Maryland, 21287, USA

<sup>10</sup>The Skip Viragh Center for Pancreatic Cancer The Johns Hopkins University School of Medicine, Baltimore, Maryland, 21287, USA

### Abstract

Pancreatic adenocarcinoma (PDA) is one of the most chemotherapy and radiotherapy resistant tumors. The c-Met and Hedgehog (Hh) pathways have been shown previously by our group to be key regulatory pathways in the primary tumor growth and metastases formation. Targeting both the HGF/c-Met and Hh pathways has shown promising results in pre-clinical studies; however, the benefits were not readily translated into to clinical trials with PDA patients. In this study, utilizing

**Corresponding author:** Correspondence and requests for materials should be addressed to L.Z., Lei Zheng, M.D., Ph.D. lzhen6@jhmi.edu, Department of Oncology, Johns Hopkins University School of Medicine, 1650 Orleans Street, CRB1, Room 488, Baltimore, MD 21287. Tel: 410-5026241; Fax: 410-6148216.

\*These authors contributed equally.

mouse models of PDA, we showed that inhibition of either HGF/c-Met or Hh pathways sensitize the PDA tumors to gemcitabine resulting in decreased primary tumor volume as well as significant reduction of metastatic tumor burden. However, prolonged treatment of single HGF/c-Met or Hh inhibitor leads to the resistance to these single inhibitors, likely because the single c-Met treatment leads to the enhanced expression of Shh, and vice versa. Targeting both the HGF/c-Met and Hh pathways simultaneously overcame the resistance to the single inhibitor treatment and led to a more potent anti-tumor effect in combination with the chemotherapy treatment.

## Keywords

Pancreatic ductal adenocarcinoma; Cancer treatment; Tumor microenvironment; c-Met pathway; Hedgehog pathway

---

## Introduction

Pancreatic adenocarcinoma (PDA) has the worst prognosis of any major malignancy, with 5-year survival of about 5% (1, 2) and is one of the most chemotherapy and radiotherapy resistant tumors (2, 3). PDA is characterized by very dense stroma that makes up anywhere from 60% to 90% of the total tumor volume (4). The stromal compartment is made up of variety of different cells and proteins that act together to develop an environment that is suppressive to the immune system, drug resistant and pro-tumorigenic (5). Although there have been numerous new therapies developed for other cancers, little progression has been made finding new therapies for PDA despite promising results from pre-clinical studies.

It is well documented that c-Met receptor and its ligand HGF are upregulated in PDA (6). Upregulation of c-Met and HGF is detected early in PDA development and promotes tumorigenesis in conjunction with other oncogenic signals (7). Because HGF is exclusively secreted by stromal fibroblasts (8) and stromal expression of HGF was correlated with decreased disease free survival (9), activation of c-Met in neoplastic cells is believed to be subject to the regulation of signals from the stroma. More recently, HGF/c-Met has been investigated as a therapeutic target for PDA. The combination of gemcitabine and crizotinib, a small molecule c-Met inhibitor, was tested in murine models and was shown to enhance the intratumoral delivery of gemcitabine and result in tumor reduction of the PDA xenograft (10). Moreover, Jin. et al. showed that antibody targeting of c-Met receptor in an orthotopic mouse model of PDA led to decreased tumor burden and prolonged survival (11). More recently, HGF/c-Met inhibitors have been tested in multiple early phase clinical trials, which have shown promising results in variety of solid cancers (10). Unfortunately, the phase II trial of cabozantinib showed minimal benefits in patients with PDA, despite promising results in subjects with other solid tumors (12, 13).

The hedgehog (Hh) pathway, specifically the activating ligand, Sonic hedgehog (Shh), is overexpressed by PDA tumor cells; however its function is restricted to the stromal compartment (14–16). It has been noted that Hh pathway activation and Smo receptor overexpression only occur in cancer-associated fibroblasts but not the neoplastic cells (17). It was subsequently reported that targeting Hh pathway in murine models of PDA depletes stroma and sensitizes primary tumors to gemcitabine, leading to tumor shrinkage (18, 19).

However, targeting the Hh pathway in patients with PDA showed no additional benefit when added to the standard of care chemotherapy treatments (20).

Though, targeting both the HGF/c-Met and Hh pathways have shown promising results in pre-clinical studies, the benefits were not readily translated into clinical trials with PDA patients (20–23). Thus, we investigated the mechanisms of resistance to the single inhibitor of HGF/c-Met or Hh pathway and determined if targeting both the HGF/c-Met and Hh pathways simultaneously would overcome the resistance to single inhibitor treatment and lead to a more potent anti-tumor effect in combination with chemotherapy treatment.

## Materials and Methods

### Cell Culture

The murine pancreatic tumor cell lines- KPC and mCAF (mouse Cancer Associated Fibroblasts) were established in accordance with the Johns Hopkins Medical Institution Institutional Review Board (JHMI IRB)-approved protocols, and obtained between 2011 and 2015, and authenticated by DNA and gene expression profiling and cultured as previously described (24, 25). Briefly, cells were maintained in RPMI 1640 medium (Gibco, Grand Island, NY, USA) supplemented with 10% FBS (Gibco), 2 mM L-glutamine (Gibco), 1% non-essential amino acids (Gibco), 1 mM sodium pyruvate (Gibco), 50 units/mL penicillin and 50 µg/mL streptomycin (Gibco). The KPC cells were grown at 37°C in 5% CO<sub>2</sub>.

### Mouse models of PDA

All animal experiments conformed to the guidelines of the Animal Care and Use Committee of the Johns Hopkins University, and animals were maintained in accordance with the guidelines of the American Association of Laboratory Animal Care. All mice were monitored twice a day.

A genetically engineered mouse model of PDA, designated KPC mice, was previously established through a knock-in of pancreatic-specific, conditional alleles of the KRAS<sup>G12D</sup> and TP53<sup>R172H</sup> mutations on a mixed 129/SvJae/C57Bl/6 background. These mice, when crossed with PDX-1-CRE<sup>+/+</sup> mice, develop PanIN lesions that progress stepwise, similar to human disease, into PDA (26).

The mouse pancreatic orthotopic model was described previously (27). In brief,  $2 \times 10^6$  KPC cells were subcutaneously injected into the flanks of syngeneic female C57Bl/6 mice. After 1 to 2 weeks, the subcutaneous tumors were harvested and cut into ~1-mm<sup>3</sup> pieces. New syngeneic female C57Bl/6 mice, ages 8 to 10 weeks, were anesthetized. The abdomen was opened via a left subcostal incision. A small pocket was prepared inside the pancreas using microscissors, into which one piece of the subcutaneous tumor was implanted. The incision in the pancreas was closed with a suture. The abdominal wall was sutured, and the skin was adapted using wound clips.

### c-Met and Hh inhibitor, and Gemcitabine treatments

For the *in vivo* studies, the Hedgehog signaling pathway inhibitor (28) NVP-LDE225 (provided by Novartis) was used at 50 mg/kg and the HGF/c-Met inhibitor INCB28060

(purchased from AbMole, Houston, TX, USA) (29, 30) was used at 1 mg/kg, both inhibitors were resuspended in DMSO. DMSO was used as a vehicle control for all treatments. The KPC and orthotopic transplant model mice were dosed daily by oral (31) gavage with NVP-LDE225, INCB28060, NVP-LDE225 + INCB28060 (at the same dose as their corresponding single inhibitor treatments) or DMSO for 7, 14 or 21 days as indicated in the treatment schemas (Figure 1, 3 and 4). *In vitro* experiments utilizing the above-mentioned inhibitors were previously described (25). Gemcitabine (Sigma-Aldrich, St. Louis, MO, USA) was reconstituted in deionized and distilled water at 20mg/ml and 100  $\mu$ l administered via intraperitoneal injection into respective mice.

### Ultrasound and tumor measurement

KPC mice of 12 to 14 weeks were examined by ultrasound using the VEVO 770 (VisualSonics, Toronto, Ontario, Canada) small animal ultrasound to confirm primary tumors. Mice bearing tumors of similar sizes were chosen for the study. Orthotopic mice were examined by ultrasound 5 days post tumor implantation to confirm the presence of the tumor and establish a baseline tumor volume. Ultrasound on the mice was performed again on day 7 of treatment in all experiments and on treatment day 14 and 21 in experiments with 14 and 21-day treatments. Tumor volume was calculated from the following formula:  $(L \text{ (long axes)} \times S^2 \text{ (short axes)})/2$ . In total, 3 images of each tumor were captured, and the image with the largest value was used to calculate the tumor volume. Tumor volume fold change was determined for each 7 days of treatment by calculating the ratio of tumor volume from week 1/baseline, week2/week1 and week3/week1.

### TUNEL assay

The TUNEL (terminal deoxynucleotidyl transferase–mediated deoxyuridine triphosphate nick end labeling) assay was performed according to the manufacturer's instructions (Roche). Briefly, the slides were baked at 62.5°C for 30 minutes to melt the paraffin. Then the slides were hydrated and proteinase K was added for 30 minutes at room temperature to expose the tissue. Following 5-minute wash in PBS, the TUNEL reaction solution was added to slides and positive control (DNase I mediated DNA breakage) and incubated for 60 minutes at 37°C, protected from light. For negative control, label solution only was added to a slide and incubated as above. Then, all slides were washed 3 times in PBS (5 minutes each wash). After the washes, converted POD was added to the slides and the slides were incubated again for 60 minutes at 37°C, protected from light. Following another 3 washes in PBS (5 minutes each), DAB was added to develop the reaction (10 minutes). Lastly, the slides were washed as above, dehydrated, mounted and subjected to analysis.

### Immunohistochemistry and Immunofluorescence

Immunohistochemistry (IHC) staining for Shh, c-Met, E-Cadherin, IGF-1 and Ki67 were performed by hand. Tissue blocks with poor quality were excluded from the study. The slides for all stainings were hydrated; antigen retrieval was performed in a pressure cooker with citrate buffer (pH 6.0) for Shh and Ki67, in a steamer with citrate buffer (pH 6.0) for c-Met and IGF-1 and with Tris-EDTA buffer (pH 9.0) for E-Cadherin. Then, the slides were blocked in peroxidase, avidin and biotin block sequentially. Goat-anti-Shh (R&D), rabbit-anti-c-Met (Santa Cruz), rabbit anti-IGF-1 (Abcam), rabbit anti-E-Cadherin (Abcam), or

rabbit anti-Ki67 (Abcam) primary antibodies at 1:50 (Shh, c-Met, E-Cadherin), 1: 500 (Ki67) and 4µg/ml (IGF-1) were added, and the slides were incubated for 1 hour at room temperature. Then, rabbit anti-goat or goat anti-rabbit biotinylated secondary antibodies (Vector Laboratories) respectively, were added for 30 minutes at room temperature. The signal was amplified and detected using the ABC Vectastain kit (Vector Laboratories) according to the manufacturer's instructions. The slides were developed using DAB and counterstained by hematoxylin. Lastly, the slides were dehydrated and mounted. All IHC slides were analyzed and scored by a pathologist. Immunofluorescence staining of c-Met and Shh was described in Supplementary Materials and Methods.

### shRNA knockdown of c-Met

Viral supernatants were produced as previously described using shRNA against mouse c-Met or scrambled shRNA control (Dharmacon) (27). Then, KPC cells were plated at 50% confluency and allowed to adhere for 24 hours. On the day of viral infection, the KPC media was aspirated and replaced with appropriately titered viral supernatant (1ml/1 well of 6 well plate) with polybrene (8 µg/ml). The infection was allowed to proceed for 24 hours. After 24-hour infection, the cells were treated with appropriate inhibitors or vehicle control for additional 24 hours. Then, the cells were harvested and Annexin V expression was analyzed as previously described (32). Knockdown of c-Met was confirmed by qRT-PCR as described below.

### Quantitative real time RT-PCR

The RNeasy Micro Kit (Qiagen Inc, Valencia, CA, USA) was used to extract total RNA from cell pellets. The RNA was then converted to cDNA using the Superscript III First Strand Synthesis Supermix Kit (Life Technology, Carlsbad, CA, USA). Quantitative real-time RT-PCR (qPCR) was performed on the StepOnePlus Real Time PCR System (Life Technology) and analyzed by the StepOne software V2.1. The expression of *c-Met*, *HGF*, and *Shh* was measured by SYBR Green-based qPCR. All gene expression was normalized to the expression of *GAPDH*. All PCR reactions were performed in triplicate. The primers used for RT-PCR are as follow:

**c-Met:** F-5'TGTCCGATACTCGTCACTGC3'

R-5'CATTTTTACGGACCCAACCA 3'(Invitrogen),

**Shh:** F-5'GGCCAAGGCATTAACTTGT

R-5' CCAATTACAACCCCGACATC3'(Invitrogen),

**GAPDH:** F-5' TTGATGGCAACAATCTCCAC3',

R-5' CGTCCCGTAGACAAAATGGT 3' (Invitrogen).

### Co-culture assay

Treatment utilizing the transwell system (BD Biosciences, San Jose, CA, USA) was performed by plating KPC cells in the bottom chamber and mCAFs in the top chamber to spatially separate the cell types. c-Met was knockdown from KPC cells whereas the mCAFs were kept in a separate 6 well plate(s) during infection. After 24-hour infection the cells

were treated in no serum media as previously described (25). After 24-hour treatment KPC cells were harvested and Annexin V analyzed.

### Statistical analysis

Statistical analysis and graphing was performed using GraphPad Prism version 6.0 software (GraphPad Software, La Jolla, CA, USA). The data are presented as the means  $\pm$  standard error of the mean (SEM). Student's t-test was used to compare differences between groups. Fisher's exact test was used to compare differences between treatment groups in the metastasis study and apoptosis study. For all analyses p value of less than 0.05 was considered statistically significant.

## Results

### Short-term inhibition of HGF/c-Met or Hh signaling enhances the sensitivity of PDA tumors to gemcitabine in transgenic and orthotopic mouse models of PDA

To understand the discrepancy in the efficacies observed between preclinical mouse studies and clinical studies of Hh inhibitors and HGF/c-Met inhibitors for treating PDAs, we examined both inhibitors in mouse models of PDA. To this end, we utilized two mouse models of PDA. The first is a genetically engineered PDA mouse model with knock-in alleles of both *Kras*<sup>G12D</sup> and *p53*<sup>R172H</sup> mutants (KPC mice), which exhibits a multi-stage tumorigenesis that progresses from normal, through PanIN lesions, to invasive and metastatic PDA (26). The second is an orthotopic implant model where tumors are grown subcutaneously from a cell line (the KPC cells) derived from KPC mice. Then tumors of similar size are implanted orthotopically into the pancreas of syngeneic mice (24). The treatment schema is shown in Figure 1A. Briefly, mice in both models were subjected to the small animal ultrasound examination to obtain baseline tumor volume. On the second day following the ultrasound, mice began daily treatment of either Hh inhibitor or HGF/c-Met inhibitor together with bi-weekly gemcitabine injection for a course of seven days. On the last day of treatment, the mice were subjected to a second ultrasound to determine tumor volume. After the ultrasound, the mice were euthanized and their pancreata were harvested for analysis. In both models, the treatment of gemcitabine alone showed a modest, however not significant decrease of primary tumor growth when compared to the vehicle treatment. Addition of Hh inhibitor to the gemcitabine resulted in a further trend of tumor shrinkage when compared to gemcitabine treatment alone. Addition of c-Met inhibitor to the gemcitabine however did not result in additional tumor shrinkage. The additional effect on tumor shrinkage observed with Hh inhibitor but not the c-Met inhibitor can be explained by the targets of the inhibitors. The Hh inhibitor affects stroma, whereas the c-Met inhibitor works predominantly on the neoplastic cells (25). The data suggest that combination of both inhibitors with gemcitabine shows a trend in shrinkage of primary tumor volume in both mouse models of PDA after one week of treatment regimen (Figure 1B, C).

To assess whether the observed tumor shrinkage is due to tumor cell death, but not a decrease in the stroma compartment, we performed terminal deoxynucleotidyl transferase (TdT) dUTP nick-end labeling (TUNEL assay) staining on the primary tumors harvested from the KPC and the orthotopic mouse models (Figure 1A) to evaluate tumor cell

apoptosis. Tumors from neither model showed significant difference in tumor cell apoptosis in the gemcitabine treatment group when compared to the vehicle treatment (Figure 2A, B). However, we observed an increased apoptosis in PDAs treated with gemcitabine in combination with c-Met inhibitor. By contrast, little enhanced apoptotic activity was seen in the tumors treated by the combination of gemcitabine and Hh inhibitor compared to gemcitabine alone, suggesting that the observed tumor shrinkage by ultrasound may represent a decrease in the stromal component. The apoptotic activity in tumors treated by gemcitabine and c-Met inhibitor was similar to that in tumors treated by gemcitabine and both inhibitors (Figure 2A, B). Taken together, following one week of treatment, there are some enhancements in anti-tumor activity by adding c-Met or Hh inhibitor or both to gemcitabine. Although the enhancement is modest in our study, it is consistent with the published preclinical studies.

### **Prolonged treatment of single HGF/c-Met or Hh inhibitor leads to resistance, which can be overcome by the combination of both c-Met and Hh inhibitors**

Next, we examined whether resistance to the c-Met and Hh inhibitors is developed after a longer course of treatment. To this end, we treated the orthotopic model for two weeks and KPC mice for three weeks. Mice in the orthotopic model could not be treated for more than 2 weeks due to the aggressive nature of this model (24, 25). We subjected those mice to ultrasound examination to obtain baseline tumor volumes. The treatment regimen was initiated on the second day following ultrasound and consisted of daily treatment of Hh inhibitor, HGF/c-Met inhibitor, or vehicle control together with bi-weekly gemcitabine administration. Second ultrasound was performed 7 days after the first one. For KPC mice, the last ultrasound was performed on the last day of 21-day treatment; and for the orthotopic model, the last ultrasound was performed on the last day of 14-day treatment (Figure 3A and Figure 4A). Interestingly, gemcitabine treatment had no effect on tumor size in the KPC mice (Figure 3B); however, it did result in significant reduction of primary tumors in the orthotopic model (Figure 4B). Gemcitabine is in the family of nucleoside analog medications, it works by blocking the creation of new DNA (33). We therefore examined the proliferation capacity of both the KPC and orthotopic tumors and showed that the activity of gemcitabine with or without Hh or c-Met inhibitor does not appear to correlate with the proliferation status of the tumors (Supplementary Figure 1). Moreover, c-Met but not Hh inhibitor further enhanced the antitumor response of gemcitabine in the KPC but not the orthotopic model. More importantly, the combination of c-Met and Hh inhibitors significantly enhanced the tumor response to gemcitabine in both the KPC and orthotopic mouse models (Figure 3B and 4B). We did not observe significant toxicities with the treatments as we did not observe any weight loss with the mice. Treatment with single target inhibitor shows no benefit in terms of tumor shrinkage (25). We observed large variability of tumor growth in the control group and the gemcitabine-alone group. This may be explained by our recent finding showing intertumoral heterogeneity of stromal signaling, namely the HGF/c-Met and Shh/IGF-1/IGF-1R pathways in mouse models of PDA (25). The large variability in growth of untreated tumors and tumors treated by gemcitabine alone may be because some tumors express high Shh signaling whereas other tumors express high c-Met signaling. However, when the tumors are treated by stroma-targeting agents, their responses to gemcitabine become more uniform. To determine the effect of the treatment regimen, we

analyzed the apoptosis of tumor cell via the TUNEL assay following more than one week of treatment. As expected, gemcitabine only group shows a minimal increase in tumor cell death when compared to the vehicle treatment (Figure 3C). Moreover, the addition of single inhibitor seems to have no effect on the incidence of apoptotic tumor cells, suggesting that the resistance to the single inhibitors is developed following a longer course (14 days or 21 days) of treatment. Importantly, only dual inhibition of both Hh and HGF/c-Met pathways shows increased sensitivity to gemcitabine as demonstrated by the significantly increased tumor cell death (Figure 3C). These results suggest that the resistance to the c-Met and Hh inhibitor is developed following a prolonged treatment of each individual inhibitor; however, the resistance may be overcome by combining both c-Met and Hh inhibitors.

Next, we wanted to determine if prolonged combination treatment of dual stromal inhibitors and gemcitabine has an effect on incidence of metastasis. We utilized the orthotopic model for this part of the study, since it allows for the establishment of primary tumors of similar size (24). We previously showed that untreated mice become morbid and die between day 17 and day 25 with a median survival of 21 days (25). Thus, following 2-week treatment (Figure 4A), we chose to stop the experiment on day 19 before the majority of mice would have died, specifically, before there were no more than two dead mice in each treatment group. We euthanized all the mice and harvested their livers, gut, lungs and peritoneum for further analysis. Gross examination followed by histological examination of the metastasis formed revealed that single stromal agents in combination with gemcitabine show a trend in the reduction of metastases formation, which is in consistent with literature reports (34, 35) (Figure 4C). Importantly, the group with dual inhibitor treatment in addition to gemcitabine showed no metastases (Figure 4C). This result suggests that the combination of c-Met and Hh inhibitors in addition to gemcitabine has significantly suppressed metastasis formation.

### **Single c-Met or Hh inhibitor treatment leads to the enhanced expression of the other target and the combination of both c-Met and Hh inhibitors suppresses the expression of both targets more effectively**

We then sought to understand the lack of effect of Hh or c-Met inhibition on primary tumor volume by examining the expression of their targets in PDAs from treated mice. We performed immunohistochemistry (IHC) staining on primary tumors from both the KPC (Figure 5A) and the orthotopic (Figure 5B) mouse models that have been treated with gemcitabine alone or in combination with the inhibitors for one week (Figure 1A). As anticipated, either single c-Met or Hh inhibitor in combination with gemcitabine lead to decrease of the c-Met and Shh expression, respectively (Figure 5; Supplementary Figure 2). However, in the mice treated with c-Met inhibitor, the expression of Shh was enhanced; and in mice treated with Hh inhibitor, the expression of c-Met was enhanced following one week of treatment. Similar results were observed in PDAs from the mice treated for three weeks (Supplementary Figure 3). These results suggest that the ineffectiveness of these inhibitors in further sensitizing PDA to the gemcitabine treatment beyond one week may be attributed to the activation of alternative pathways. Consistent with this notion, inhibition of both c-Met and Hh pathways along with gemcitabine treatment shows a decrease in the expression of both c-Met and Shh when compared to the gemcitabine alone treatment group.



## Compensatory overexpression/activation of alternative pathways may account for single target resistance in PDA

To further investigate the mechanism of resistance to gemcitabine in combination with one inhibitor, we first examined the effect of Shh inhibitor and c-Met inhibitor on KPC tumor cells and mouse cancer associated fibroblast (mCAF) cells, respectively. As shown in Figure 6A, Shh inhibitor decreased the expression of Shh, but increased the expression of *HGF* from mCAF cells. In addition, c-Met inhibitor decreased the expression of *c-Met*, but increased the expression of *Shh* from the KPC tumor cells. This result suggests that when Shh is inhibited, the HGF/c-Met pathway is activated as a compensation; and when c-Met is inhibited, the Shh expression is induced. Second, we confirmed that inhibition of c-Met and/or Shh via the pharmaceutical agents utilized in the study, leads to blockade of their respective pathways by analyzing downstream targets of each pathway (Figure 6B and C). Our recently published study placed IGF-1 downstream of Shh (25). Analysis of IGF-1 expression in PDA tumors from orthotopic mouse model confirmed that expression of the protein is decreased in samples treated with Hh inhibitor but not in the c-Met treated samples when compared to vehicle control. As expected, combination treatment resulted in decreased expression of IGF-1. Moreover, no difference in the amount of IGF-1 was noted between the vehicle control and gemcitabine groups (Figure 6B). E-cadherin is downstream of both HGF/c-Met and Shh pathways (5, 25, 36) therefore, either inhibitor was able to activate E-cadherin. When both inhibitors were used, the expression of E-cadherin was higher than that seen with single inhibitors (Figure 6C). Third, we tested the selectivity of c-Met inhibitor utilizing tumor cells with c-Met knockdown by shRNA. As shown in Table 1, when c-Met is knockdown (Supplementary Figure 4A), c-Met inhibitor is no longer capable of increasing apoptosis, although c-Met knockdown itself can induce apoptosis. Interestingly, Shh inhibitor also failed to increase the apoptotic rate in cells with c-Met knockdown, suggesting that the effect of the combination of c-Met and Shh inhibitors also depends on c-Met. Moreover, this finding suggests that c-Met can not only mediate the effect of Hh but it also implies that knockdown and small molecule targeting of c-Met have different effect on Shh expression (Figure 6A and Supplemental Figure 4B).

## Discussion

PDA is still one of the deadliest cancers worldwide with limited therapeutic options (2). Here, we demonstrate that combination of targeted stromal pathway inhibition of the c-Met and Hh pathways along with gemcitabine treatment lead to significant reduction of primary tumor volume and diminished metastases formation in mouse models of PDA. We also provide evidence that this dual stromal therapy overcomes single agent resistance and increases gemcitabine sensitivity.

This study not only confirms the prior finding but also provides an additional mechanistic explanation to the affectivity of dual stromal inhibition in terms of the decrease in PDA tumor burden. It also explains why single stromal agent clinical trials fail to show efficacy in human subjects (37). One of the reasons is the development of resistance to those agents by overexpression of other, non-targeted pathways. We demonstrated that the upregulation of

those non-targeted pro-tumorigenic pathways tends to be more prominent in longer-term treatments.

The use of PDA mouse models though very informative, has some limitations. Mice with implanted tumors have a very short life span (~3 weeks) without treatments; thus we used the “two weeks” treatment course to mimic the long course of treatment. Although KPC spontaneous tumor models could be treated for a longer course, we found that the mice could not tolerate a prolonged course of treatment with daily oral gavage and were concerned about inadvertent effect from oral gavage. Those limitations lead to difficulty in accessing survival benefit in these studies. Nevertheless, the data presented in these studies support further testing of the combination of Hh and c-Met inhibitors in clinical trials.

Numerous studies reported the benefit of stromal modulation in enhancing chemo sensitivity in mouse models of PDA (19, 38–41), however the use of Hh inhibitor in combination with chemotherapy agents in clinical trials with human subjects failed to show benefit (20–23). The importance of Hh and c-Met pathways as potential PDA targets has been well documented (25, 42–44). The role of Hh signaling in PDA has been rather controversial. Some studies show that targeting the pathway is beneficial in PDA (45) whereas others documented that activation of Hh signaling can slow tumorigenesis (46). We recently published a study showing that expression of Shh and HGF is heterogeneous in the tumor microenvironment of PDA and only blockade of both pathways has a beneficial effect on metastasis of PDA (25). This current study offers an insight into the lack of success of trials as well it begins to answer the opposing reports in current literature on the role of Hh pathway by showing that combinational targeted therapy results in PDA tumor sensitization to gemcitabine and overcomes the resistance mechanism of single agent targeted therapies. Targeting c-Met with cabozantinib was shown to increase gemcitabine efficacy on cultured pancreatic tumor cells. The fact that cabozantinib reduced stem cell markers and also self-renewal potential of PDA cells may account for the mechanism of inhibition of c-Met in overcoming the resistance of PDA to chemotherapy (43, 44). Our recent study described the role of stroma in c-Met inhibition (25), which provides a separate mechanism to overcoming resistance to chemotherapy, although we show that inhibition of c-Met is compensated by increased levels of another stromal pathway, namely the Hh pathway. Since Hh signaling is also involved in self-renewal of PDA, it is possible that the combination of Hh and c-Met inhibition overcomes the resistance in PDA to gemcitabine through inhibiting the self-renewal potential of PDA. Further studies are warranted to determine the exact molecular mechanism underlying the role of c-Met and Hh signaling in chemotherapy resistance in PDA.

## Supplementary Material

Refer to Web version on PubMed Central for supplementary material.

## Acknowledgments

**Financial Information:** This work was supported in part by NIH R01 CA169702 (L.Zheng), NIH K23 CA148964-01 (L.Zheng), Viragh Foundation and the Skip Viragh Pancreatic Cancer Center at Johns Hopkins

(E.M.Jaffee, L.Zheng), Lefkofsky Family Foundation (L.Zheng), the NCI SPORE in Gastrointestinal Cancers P50 CA062924 (E.M.Jaffee, L.Zheng) and a Lustgarten Foundation (L.Zheng) grant.

## References

1. Bond-Smith G, Banga N, Hammond TM, Imber CJ. Pancreatic adenocarcinoma. *Bmj*. 2012; 344:e2476. [PubMed: 22592847]
2. Siegel R, Ma J, Zou Z, Jemal A. Cancer statistics, 2014. *CA Cancer J Clin*. 2014; 64:9–29. [PubMed: 24399786]
3. Warshaw AL, Fernandez-del Castillo C. Pancreatic carcinoma. *The New England journal of medicine*. 1992; 326:455–65. [PubMed: 1732772]
4. Maitra A, Hruban RH. Pancreatic cancer. *Annual review of pathology*. 2008; 3:157–88.
5. Rucki AA, Zheng L. Pancreatic cancer stroma: understanding biology leads to new therapeutic strategies. *World J Gastroenterol*. 2014; 20:2237–46. [PubMed: 24605023]
6. Jones S, Zhang X, Parsons DW, Lin JC, Leary RJ, Angenendt P, et al. Core signaling pathways in human pancreatic cancers revealed by global genomic analyses. *Science (New York, NY.)*. 2008; 321:1801–6.
7. Yu J, Ohuchida K, Mizumoto K, Ishikawa N, Ogura Y, Yamada D, et al. Overexpression of c-met in the early stage of pancreatic carcinogenesis; altered expression is not sufficient for progression from chronic pancreatitis to pancreatic cancer. *World journal of gastroenterology : WJG*. 2006; 12:3878–82. [PubMed: 16804974]
8. Ide T, Kitajima Y, Miyoshi A, Ohtsuka T, Mitsuno M, Ohtaka K, et al. Tumor-stromal cell interaction under hypoxia increases the invasiveness of pancreatic cancer cells through the hepatocyte growth factor/c-Met pathway. *International journal of cancer Journal international du cancer*. 2006; 119:2750–9. [PubMed: 16998831]
9. Ide T, Kitajima Y, Miyoshi A, Ohtsuka T, Mitsuno M, Ohtaka K, et al. The hypoxic environment in tumor-stromal cells accelerates pancreatic cancer progression via the activation of paracrine hepatocyte growth factor/c-Met signaling. *Annals of surgical oncology*. 2007; 14:2600–7. [PubMed: 17534684]
10. Avan A, Caretti V, Funel N, Galvani E, Maftouh M, Honeywell RJ, et al. Crizotinib inhibits metabolic inactivation of gemcitabine in c-Met-driven pancreatic carcinoma. *Cancer research*. 2013; 73:6745–56. [PubMed: 24085787]
11. Jin H, Yang R, Zheng Z, Romero M, Ross J, Bou-Reslan H, et al. MetMAB, the one-armed 5D5 anti-c-Met antibody, inhibits orthotopic pancreatic tumor growth and improves survival. *Cancer research*. 2008; 68:4360–8. [PubMed: 18519697]
12. Yap TA, Olmos D, Brunetto AT, Tunariu N, Barriuso J, Riisnaes R, et al. Phase I trial of a selective c-MET inhibitor ARQ 197 incorporating proof of mechanism pharmacodynamic studies. *Journal of clinical oncology : official journal of the American Society of Clinical Oncology*. 2011; 29:1271–9. [PubMed: 21383285]
13. Sharma N, Adjei AA. In the clinic: ongoing clinical trials evaluating c-MET-inhibiting drugs. *Therapeutic advances in medical oncology*. 2011; 3:S37–50. [PubMed: 22128287]
14. Tian H, Callahan CA, DuPree KJ, Darbonne WC, Ahn CP, Scales SJ, et al. Hedgehog signaling is restricted to the stromal compartment during pancreatic carcinogenesis. *Proceedings of the National Academy of Sciences of the United States of America*. 2009; 106:4254–9. [PubMed: 19246386]
15. Li X, Ma Q, Duan W, Liu H, Xu H, Wu E. Paracrine sonic hedgehog signaling derived from tumor epithelial cells: a key regulator in the pancreatic tumor microenvironment. *Critical reviews in eukaryotic gene expression*. 2012; 22:97–108. [PubMed: 22856428]
16. Bailey JM, Swanson BJ, Hamada T, Eggers JP, Singh PK, Caffery T, et al. Sonic hedgehog promotes desmoplasia in pancreatic cancer. *Clinical cancer research : an official journal of the American Association for Cancer Research*. 2008; 14:5995–6004. [PubMed: 18829478]
17. Walter K, Omura N, Hong SM, Griffith M, Vincent A, Borges M, et al. Overexpression of smoothed activates the sonic hedgehog signaling pathway in pancreatic cancer-associated

- fibroblasts. *Clinical cancer research : an official journal of the American Association for Cancer Research*. 2010; 16:1781–9. [PubMed: 20215540]
18. Khan S, Ebeling MC, Chauhan N, Thompson PA, Gara RK, Ganju A, et al. Ormeloxifene suppresses desmoplasia and enhances sensitivity of gemcitabine in pancreatic cancer. *Cancer research*. 2015; 75:2292–304. [PubMed: 25840985]
  19. Olive KP, Jacobetz MA, Davidson CJ, Gopinathan A, McIntyre D, Honess D, et al. Inhibition of Hedgehog signaling enhances delivery of chemotherapy in a mouse model of pancreatic cancer. *Science (New York, NY)*. 2009; 324:1457–61.
  20. Kim EJ, Sahai V, Abel EV, Griffith KA, Greenson JK, Takebe N, et al. Pilot clinical trial of hedgehog pathway inhibitor GDC-0449 (vismodegib) in combination with gemcitabine in patients with metastatic pancreatic adenocarcinoma. *Clinical cancer research : an official journal of the American Association for Cancer Research*. 2014; 20:5937–45. [PubMed: 25278454]
  21. Pant S, Saleh M, Bendell J, Infante JR, Jones S, Kurkjian CD, et al. A phase I dose escalation study of oral c-MET inhibitor tivantinib (ARQ 197) in combination with gemcitabine in patients with solid tumors. *Annals of oncology : official journal of the European Society for Medical Oncology / ESMO*. 2014; 25:1416–21.
  22. Catenacci DV, Junttila MR, Karrison T, Bahary N, Horiba MN, Nattam SR, et al. Randomized Phase Ib/II Study of Gemcitabine Plus Placebo or Vismodegib, a Hedgehog Pathway Inhibitor, in Patients With Metastatic Pancreatic Cancer. *Journal of clinical oncology : official journal of the American Society of Clinical Oncology*. 2015
  23. Michaud NR, Wang Y, McEachern KA, Jordan JJ, Mazzola AM, Hernandez A, et al. Novel neutralizing hedgehog antibody MEDI-5304 exhibits antitumor activity by inhibiting paracrine hedgehog signaling. *Molecular cancer therapeutics*. 2014; 13:386–98. [PubMed: 24344235]
  24. Foley K, Rucki AA, Xiao Q, Zhou D, Leubner A, Mo G, et al. Semaphorin 3D autocrine signaling mediates the metastatic role of annexin A2 in pancreatic cancer. *Science signaling*. 2015; 8 ra77.
  25. Rucki AA, Foley K, Zhang P, Xiao Q, Kleponis J, Wu AA, et al. Heterogeneous Stromal Signaling within the Tumor Microenvironment Controls the Metastasis of Pancreatic Cancer. *Cancer research*. 2017; 77:41–52. [PubMed: 27821486]
  26. Hingorani SR, Wang L, Multani AS, Combs C, Deramaudt TB, Hruban RH, et al. Trp53R172H and KrasG12D cooperate to promote chromosomal instability and widely metastatic pancreatic ductal adenocarcinoma in mice. *Cancer Cell*. 2005; 7:469–83. [PubMed: 15894267]
  27. Zheng L, Foley K, Huang L, Leubner A, Mo G, Olinio K, et al. Tyrosine 23 phosphorylation-dependent cell-surface localization of annexin A2 is required for invasion and metastases of pancreatic cancer. *PloS one*. 2011; 6:e19390. [PubMed: 21572519]
  28. Pan S, Wu X, Jiang J, Gao W, Wan Y, Cheng D, et al. Discovery of NVP-LDE225, a Potent and Selective Smoothed Antagonist. *ACS medicinal chemistry letters*. 2010; 1:130–4. [PubMed: 24900187]
  29. Liu X, Wang Q, Yang G, Marando C, Koblisch HK, Hall LM, et al. A novel kinase inhibitor, INCB28060, blocks c-MET-dependent signaling, neoplastic activities, and cross-talk with EGFR and HER-3. *Clinical cancer research : an official journal of the American Association for Cancer Research*. 2011; 17:7127–38. [PubMed: 21918175]
  30. Weng LQL, Zhou J, Liu P. Pan Y inventors, Incyte Corporation, assignee. Salts of 2-fluoro-N-methyl-4-[7-(quinolin-6-yl-methyl)-imidazo[1,2-b][1,2,4]triazin-2-yl]benzamide and processes related to preparing the same. Europe patent WO. 2009 2009143211.
  31. Al-Muhsen S, Letuve S, Vazquez-Tello A, Pureza MA, Al-Jahdali H, Bahammam AS, et al. Th17 cytokines induce pro-fibrotic cytokines release from human eosinophils. *Respiratory research*. 2013; 14:34. [PubMed: 23496774]
  32. Black CM, Armstrong TD, Jaffee EM. Apoptosis-regulated low-avidity cancer-specific CD8(+) T cells can be rescued to eliminate HER2/neu-expressing tumors by costimulatory agonists in tolerized mice. *Cancer immunology research*. 2014; 2:307–19. [PubMed: 24764578]
  33. Burris HA 3rd, Moore MJ, Andersen J, Green MR, Rothenberg ML, Modiano MR, et al. Improvements in survival and clinical benefit with gemcitabine as first-line therapy for patients with advanced pancreas cancer: a randomized trial. *J Clin Oncol*. 1997; 15:2403–13. [PubMed: 9196156]

34. Ogunwobi OO, Puszyk W, Dong HJ, Liu C. Epigenetic upregulation of HGF and c-Met drives metastasis in hepatocellular carcinoma. *PLoS one*. 2013; 8:e63765. [PubMed: 23723997]
35. Hanna A, Shevde LA. Hedgehog signaling: modulation of cancer properties and tumor microenvironment. *Molecular cancer*. 2016; 15:24. [PubMed: 26988232]
36. Penchev VR, Rasheed ZA, Maitra A, Matsui W. Heterogeneity and targeting of pancreatic cancer stem cells. *Clin Cancer Res*. 2012; 18:4277–84. [PubMed: 22896694]
37. Kundranda M, Kachaamy T. Promising new therapies in advanced pancreatic adenocarcinomas. *Future oncology (London, England)*. 2014; 10:2629–41.
38. Quint K, Tonigold M, Di Fazio P, Montalbano R, Lingelbach S, Ruckert F, et al. Pancreatic cancer cells surviving gemcitabine treatment express markers of stem cell differentiation and epithelial-mesenchymal transition. *International journal of oncology*. 2012; 41:2093–102. [PubMed: 23026911]
39. Huang FT, Zhuan-Sun YX, Zhuang YY, Wei SL, Tang J, Chen WB, et al. Inhibition of hedgehog signaling depresses self-renewal of pancreatic cancer stem cells and reverses chemoresistance. *International journal of oncology*. 2012; 41:1707–14. [PubMed: 22923052]
40. Bahra M, Kamphues C, Boas-Knoop S, Lippert S, Esendik U, Schuller U, et al. Combination of hedgehog signaling blockage and chemotherapy leads to tumor reduction in pancreatic adenocarcinomas. *Pancreas*. 2012; 41:222–9. [PubMed: 22076568]
41. Noguchi K, Eguchi H, Konno M, Kawamoto K, Nishida N, Koseki J, et al. Susceptibility of pancreatic cancer stem cells to reprogramming. *Cancer science*. 2015; 106:1182–7. [PubMed: 26298849]
42. Onishi H, Katano M. Hedgehog signaling pathway as a new therapeutic target in pancreatic cancer. *World journal of gastroenterology*. 2014; 20:2335–42. [PubMed: 24605030]
43. Hage C, Rausch V, Giese N, Giese T, Schonsiegel F, Labsch S, et al. The novel c-Met inhibitor cabozantinib overcomes gemcitabine resistance and stem cell signaling in pancreatic cancer. *Cell death & disease*. 2013; 4:e627. [PubMed: 23661005]
44. Li C, Wu JJ, Hynes M, Dosch J, Sarkar B, Welling TH, et al. c-Met is a marker of pancreatic cancer stem cells and therapeutic target. *Gastroenterology*. 2011; 141:2218–27. e5. [PubMed: 21864475]
45. Thayer SP, di Magliano MP, Heiser PW, Nielsen CM, Roberts DJ, Lauwers GY, et al. Hedgehog is an early and late mediator of pancreatic cancer tumorigenesis. *Nature*. 2003; 425:851–6. [PubMed: 14520413]
46. Lee JJ, Perera RM, Wang H, Wu DC, Liu XS, Han S, et al. Stromal response to Hedgehog signaling restrains pancreatic cancer progression. *Proceedings of the National Academy of Sciences of the United States of America*. 2014; 111:E3091–100. [PubMed: 25024225]

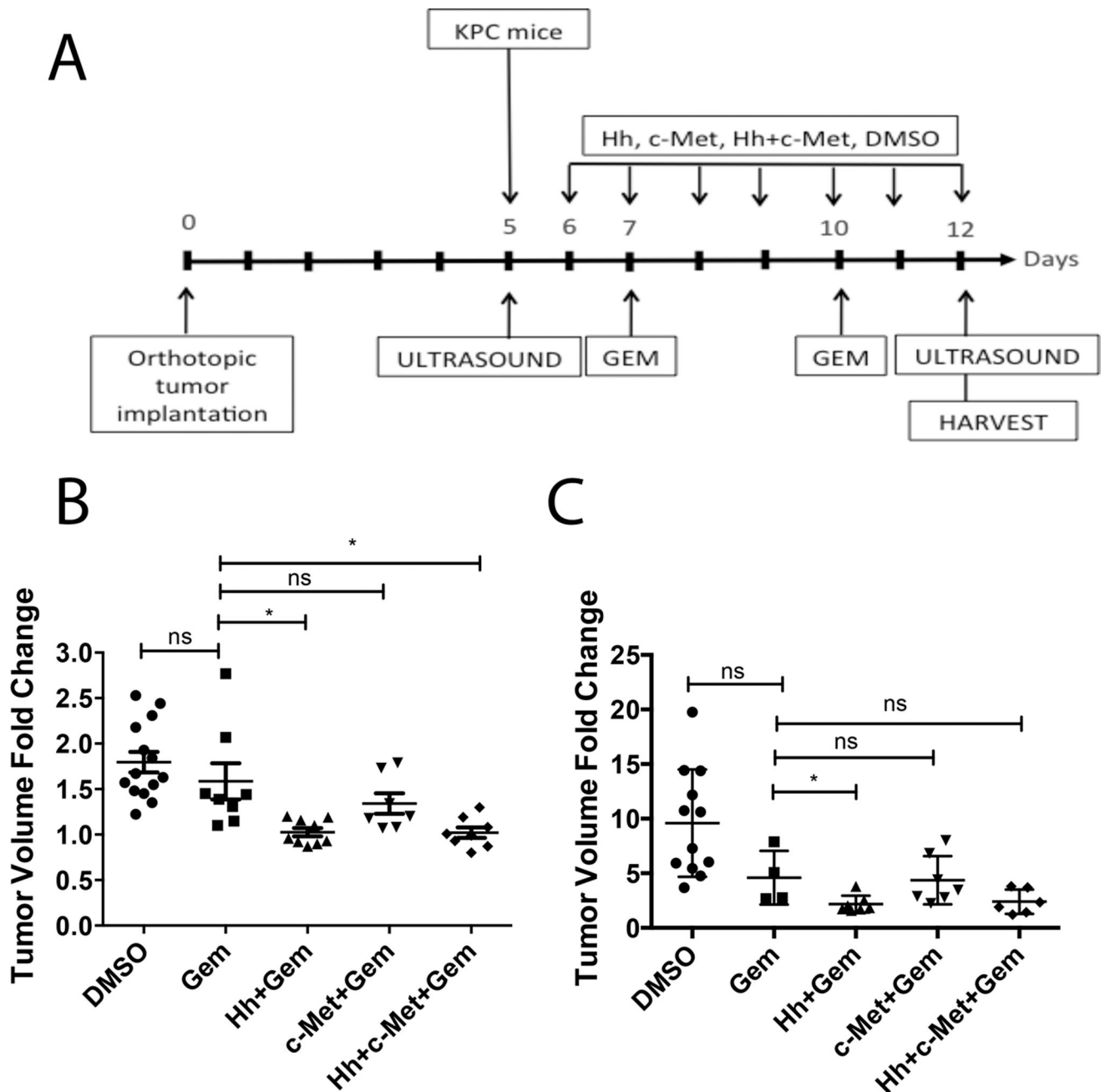


**Figure 1. Short-term inhibition of HGF/c-Met or Hh signaling enhances the sensitivity of PDA tumors to gemcitabine in transgenic and orthotopic mouse models of PDA**

**A.** Schematic representation of 1-week treatment regimen in the transgenic (KPC) and orthotopic mouse models of PDA. Day 0 represents the day of the orthotopic implantation of primary pancreatic tumors. Mice in the orthotopic model were subjected to ultrasound on postoperative day 5 to establish baseline tumor data. Daily treatment by oral gavage with inhibitor(s) or vehicle control was initiated on the day after ultrasound. In the KPC mouse model, ultrasound was performed 1 day prior to treatment initiation. In both models gemcitabine was administered bi-weekly by intraperitoneal injection. Second ultrasound was performed on the last day of treatment. Mice from all groups were euthanized on the last day

of treatment and the pancreata and livers were harvested for analysis. **B and C.** The KPC (panel B) and orthotopic (panel C) mouse models of PDA were treated with daily Hh and/or HGF/c-Met inhibitors and bi-weekly gemcitabine as shown in Panel A. Tumor volumes were obtained at baseline and on the last day of treatment. The data show tumor volume fold changes calculated as a ratio by comparison of the post-treatment tumor volume to the baseline tumor volume. Data is representative of 1 experiment. Mice that died before the completion of the planned treatment or whose quality of tumor was not adequate for analysis due to necrosis were excluded. ns- not significant \* $p < 0.05$ , \*\* $p < 0.01$ , Gem-gemcitabine (n=8), Hh-Hh inhibitor + Gem (n=9), c-Met- HGF/c-Met inhibitor + Gem (n=7), DMSO-vehicle control (n=14), Hh+c-Met+Gem (n=8). \*\*\* $p < 0.001$ , \*\*\*\* $p < 0.0001$  (unpaired student t-test).

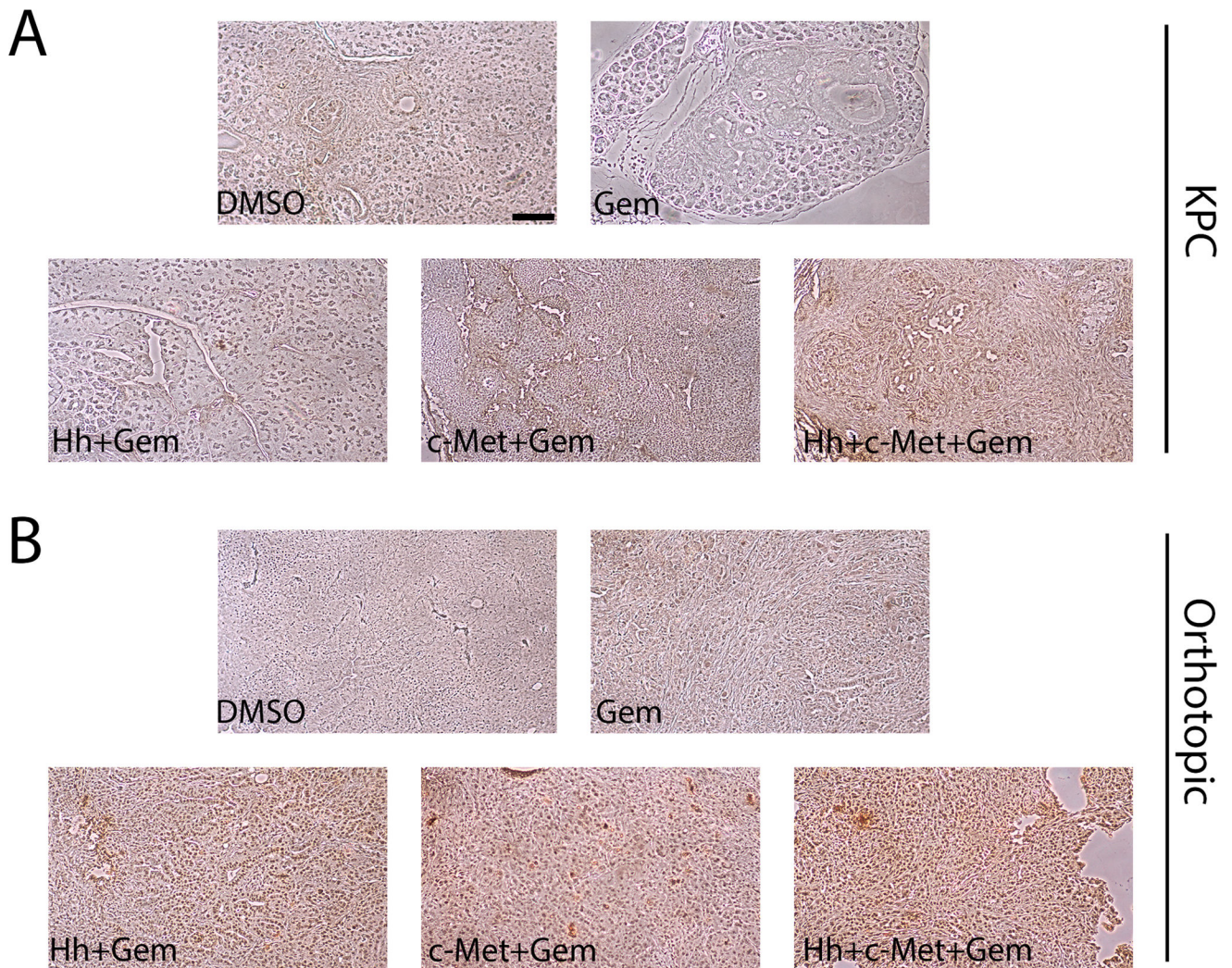


**Figure 2. Combination of Hh and/or HGF/c-Met inhibitor(s) with gemcitabine in short term treatment regimen results in enhancement tumoral cell death in the transgenic (KPC) and orthotopic mouse models**

**A and B.** The KPC (panel A) and orthotopic (panel B) mouse models of PDA were treated with Hh and/or HGF/c-Met inhibitor(s) and bi-weekly gemcitabine as shown in Figure 1A. Primary tumors from both mouse models were harvested on the last day of treatment and subjected to TUNEL staining for apoptotic cells. Representative images for each treatment group in both models are shown. The images are representative of 1 experiment. Mice that died before the completion of the planned treatment or whose quality of tumor was not adequate for analysis due to necrosis were excluded. Gem-gemcitabine (n=8), Hh-Hh inhibitor + Gem (n=9), c-Met- HGF/c-Met inhibitor + Gem (n=7), DMSO-vehicle control (n=14), Hh+c-Met+Gem (n=8). Scale bars, 200 μm.



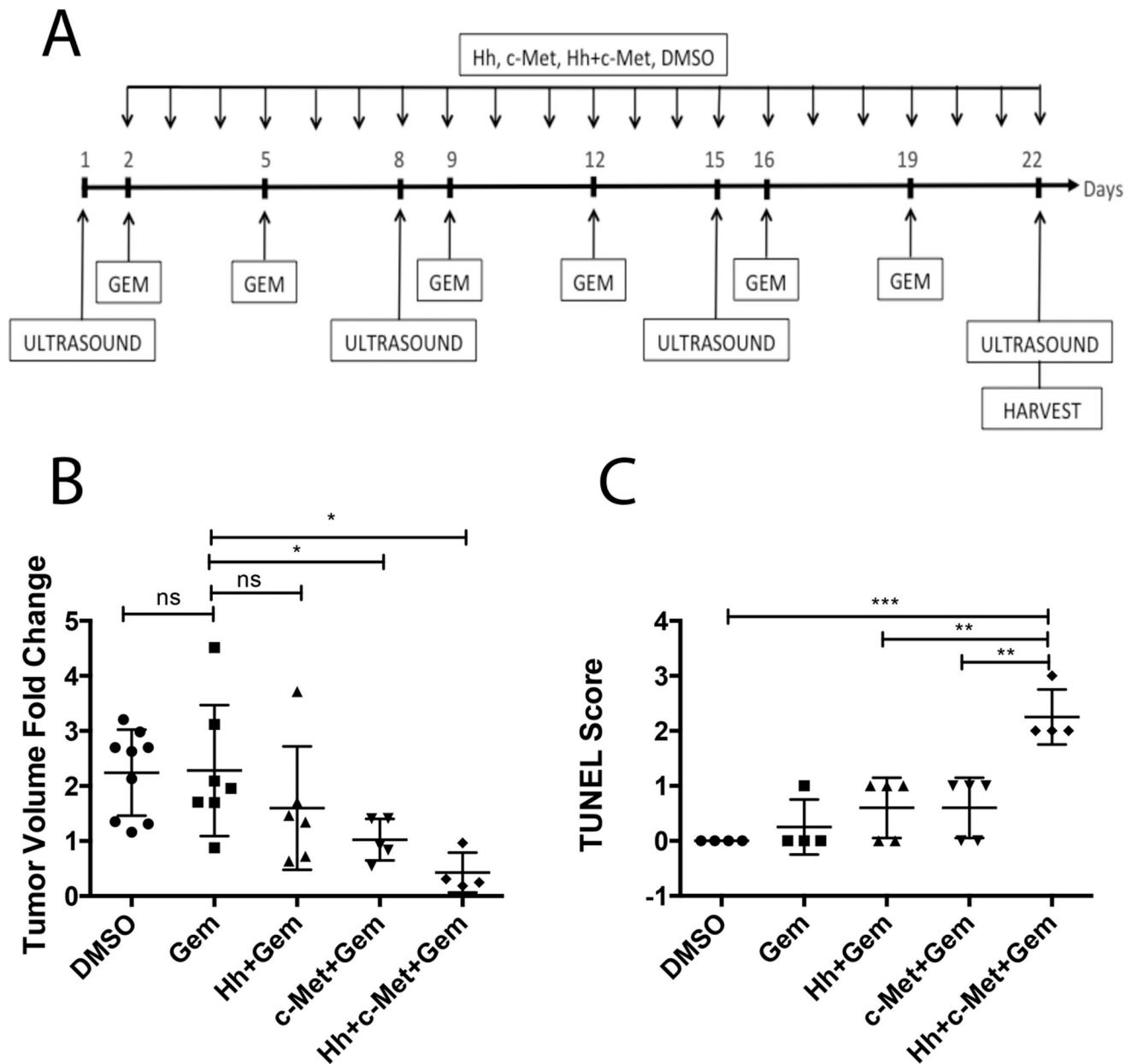


**Figure 3. Prolonged combination treatment of transgenic mouse model (KPC) with Hh and HGF/c-Met inhibitors in combination with gemcitabine leads to reduction in primary tumor volume and increased apoptosis**

**A.** Schematic representation of three-week treatment regimen in the KPC mouse model of PDA. Baseline tumor volume was determined one day before treatment, following by weekly ultrasounds until the last day of treatment. Mice were treated daily by oral gavage with Hh and/or HGF/c-Met inhibitors or vehicle control. Gemcitabine was administered bi-weekly via intraperitoneal injection. **B.** The change in tumor volume (calculated as ratio between week 3 and baseline tumor volume) is shown. **C.** Semi-quantification of TUNEL staining for apoptotic cells in KPC mouse model after 3 weeks of treatment (as shown in panel A). The scoring method used score between 0 and 3, where 0 is no positive staining and 3 is high positive staining. The data is representative of 1 experiment. Mice that died

before the completion of the planned treatment or whose quality of tumor was not adequate for analysis due to necrosis were excluded. Gem-gemcitabine (n=7), Hh-Hh inhibitor + Gem (n=6), c-Met- HGF/c-Met inhibitor + Gem (n=5), DMSO-vehicle control (n=9), Hh+c-Met +Gem (n=4).. ns- not significant \*p<0.05, \*\*p<0.01, \*\*\*p<0.001, \*\*\*\*p<0.0001 (unpaired student t-test).

Author Manuscript

Author Manuscript

Author Manuscript

Author Manuscript

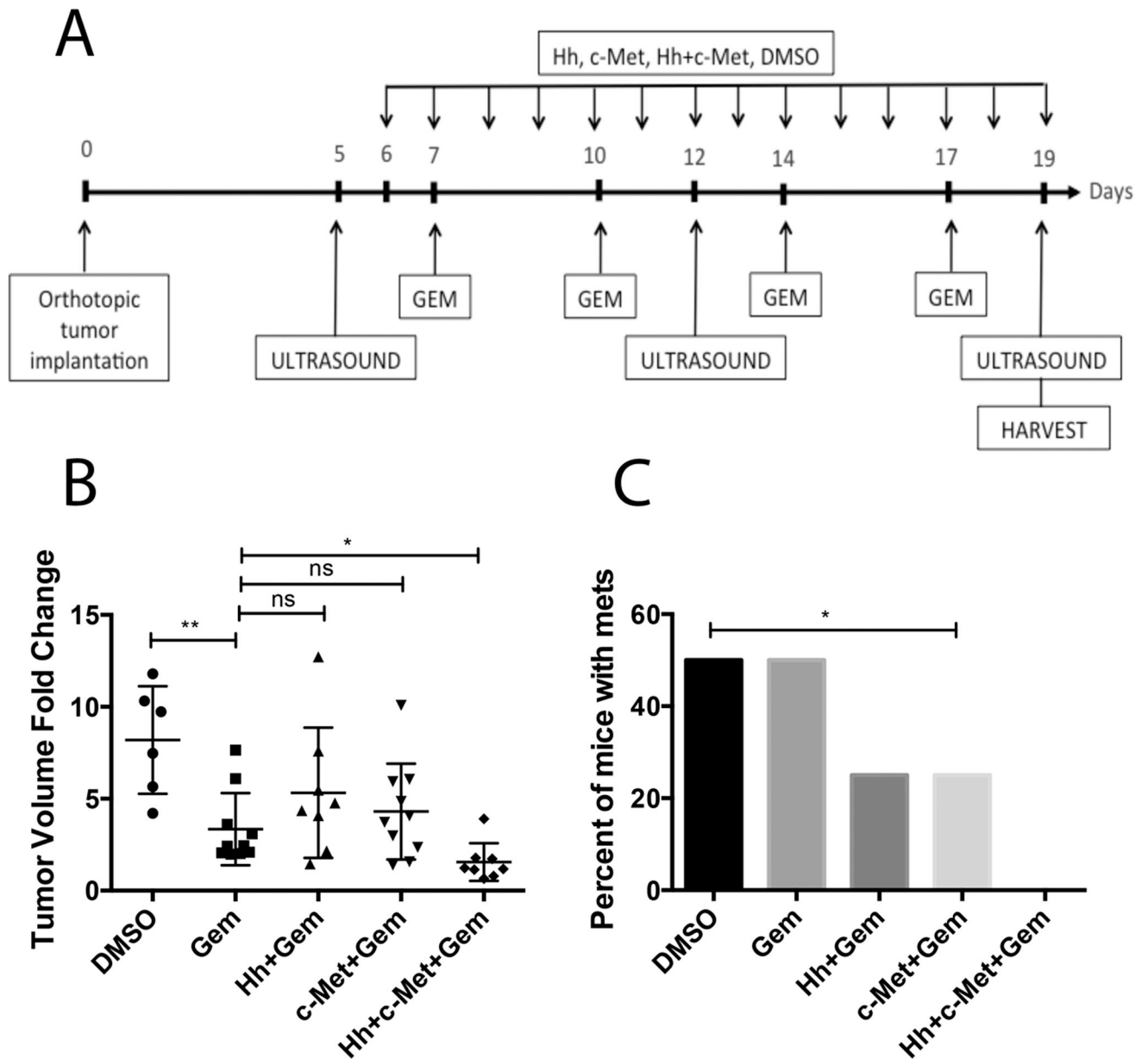


**Figure 4. Prolonged combination treatment of orthotopic mouse model with Hh and HGF/c-Met inhibitors in combination gemcitabine leads to reduction in primary tumor volume and metastatic burden**

**A.** Schematic representation of two-week treatment regimen in the orthotopic mouse model of PDA. Baseline tumor volume was determined on postoperative day 5, following by weekly ultrasounds until the last day of treatment. Mice were treated daily beginning one day after the first ultrasound by oral gavage with Hh and/or HGF/c-Met inhibitors or vehicle control. Gemcitabine was administered bi-weekly via intraperitoneal injection. In the metastasis study (panel C) livers, lungs, gut and peritoneum were harvested for gross and histological analysis of metastases. **B.** The change in tumor volume (calculated as ratio between week 3 and baseline tumor volume) is shown. Data is representative of 1 experiment. **C.** Summary of total numbers of metastases formed (gross and histological) in

each group. The data is representative of 1 experiment. Mice that died before the completion of the planned treatment or whose quality of tumor was not adequate for analysis due to necrosis were excluded. Gem-gemcitabine (n=7), Hh-Hh inhibitor + Gem (n=8), c-Met-HGF/c-Met inhibitor + Gem (n=10), DMSO-vehicle control (n=6), Hh+c-Met+Gem (n=8).. ns- not significant \*p<0.05, \*\*p<0.01, \*\*\*p<0.001, \*\*\*\*p<0.0001 (unpaired student t-test in panel B and Fisher's exact test in panel C).

Author Manuscript

Author Manuscript

Author Manuscript

Author Manuscript

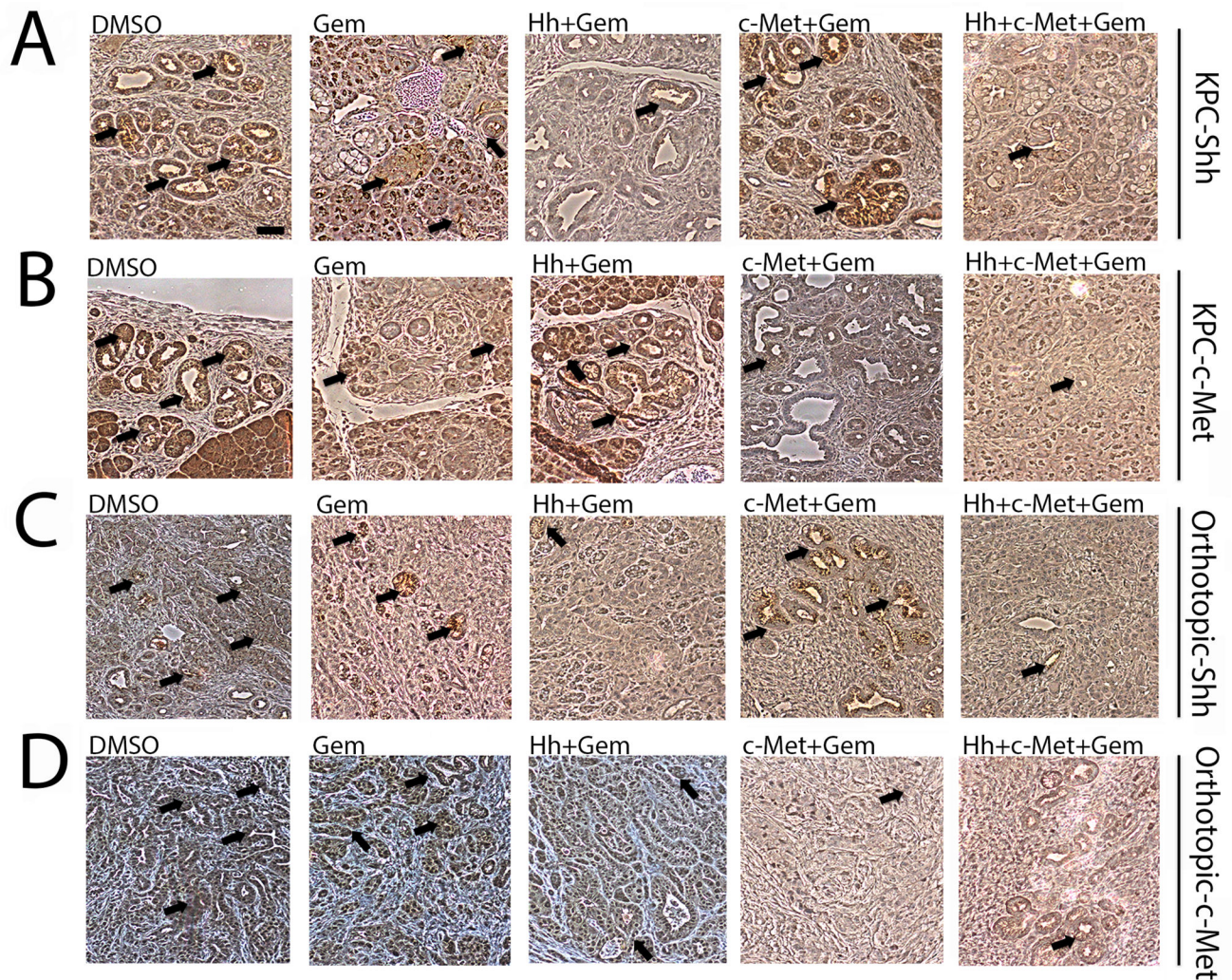


**Figure 5. Single c-Met or Hh inhibitor treatment leads to the enhanced expression of the other target and the combination of both c-Met and Hh inhibitors suppresses the expression of both targets more effectively**

**A and B.** Representative IHC images of primary tumors from the transgenic mouse model KPC stained for expression of Shh (panel A) and c-Met (panel B) showing upregulation of Shh in the c-Met treatment group and vice versa, that can be overcome by combination treatment of Hh and c-Met inhibitors with gemcitabine. **C and D.** Representative IHC images of primary tumors from the orthotopic mouse model stained for expression of Shh (panel C) and c-Met (panel D) showing upregulation of Shh in the c-Met treatment group and vice versa, that can be overcome by combination treatment of Hh and c-Met inhibitors with gemcitabine. Mice in both models were treated for 1 week (as shown in Figure 1A). The data is representative of 1 experiment. Mice that died before the completion of the planned treatment or whose quality of tumor was not adequate for analysis due to necrosis were excluded. Arrows point to positive staining. Gem-gemcitabine (n=8), Hh-Hh inhibitor + Gem (n=9), c-Met- HGF/c-Met inhibitor + Gem (n=7), DMSO-vehicle control (n=9), Hh +c-Met+Gem (n=8).. Scale bars, 200  $\mu$ m.

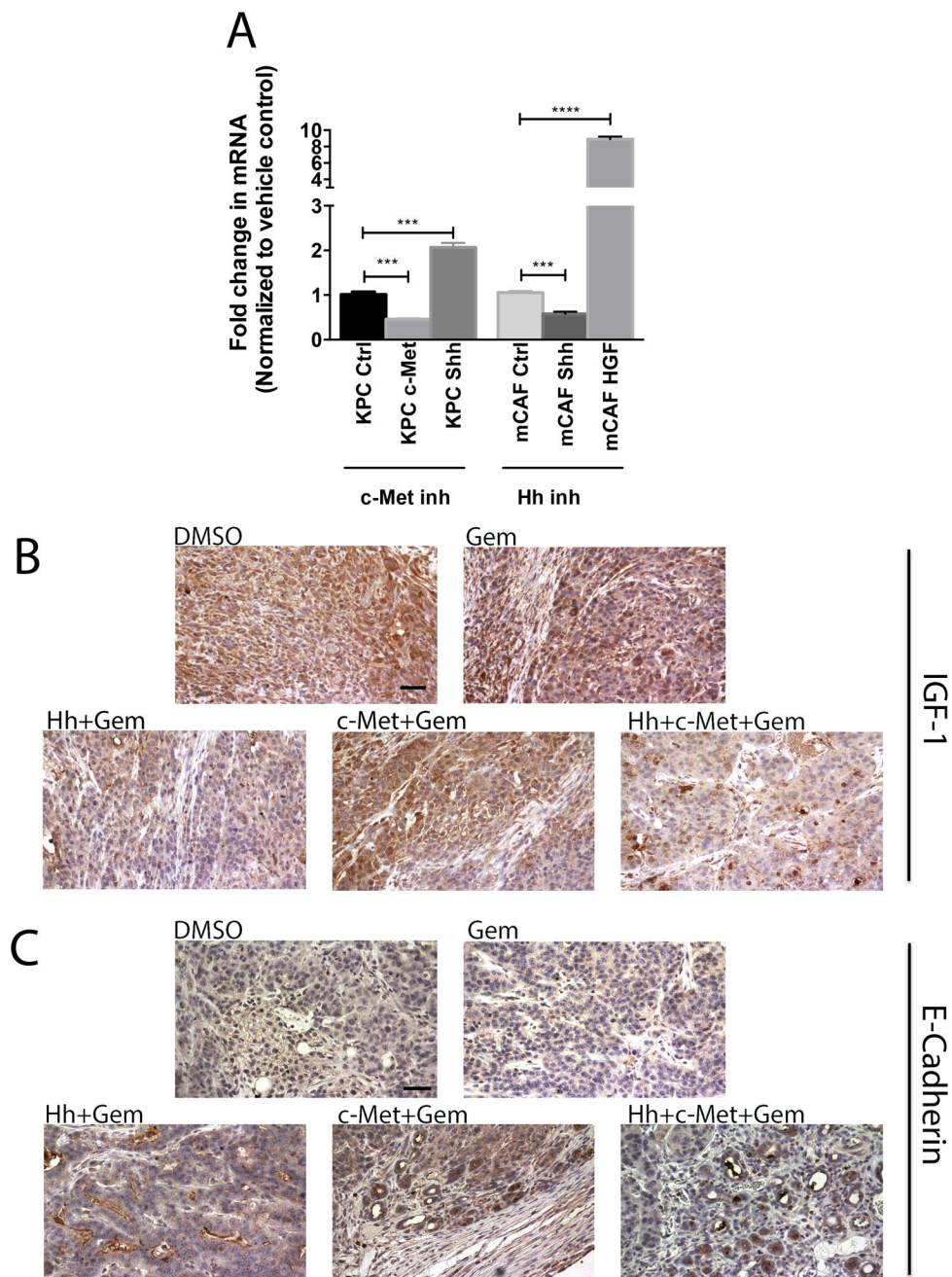


**Figure 6. Compensatory overexpression/activation of alternative pathways explains single target resistance in PDA**

A. qRT-PCR analysis of *c-Met*, *Shh* and *GAPDH* (control) in KPC tumor cells after c-Met inhibitor treatment and qRT-PCR analysis of *Shh*, *HGF* and *GAPDH* (control) in mCAFs after Hh inhibitor treatment. The gene was normalized to *GAPDH* and is shown as a fold change. B and C. Representative IHC images of primary tumors from the orthotopic mouse model stained for expression of IGF-1 (panel B) and E-Cadherin (panel C). Mice were treated for 1 week (as shown in Figure 1A). The data is representative of 1 experiment. Mice that died before the completion of the planned treatment or whose quality of tumor was not adequate for analysis due to necrosis were excluded. Gem-gemcitabine (n=8), Hh-Hh

inhibitor + Gem (n=9), c-Met- HGF/c-Met inhibitor + Gem (n=7), DMSO-vehicle control (n=9), Hh+c-Met+Gem (n=8). Scale bars, 200  $\mu$ m.

Author Manuscript

Author Manuscript

Author Manuscript

Author Manuscript

**Table 1**

Summary of the rate of apoptosis in KPC cells with/without c-Met knockdown after inhibitor treatment.

c-Met status	Treatment group	Percentage of Annexin V positive cells (+/- SEM)
shRNA-Ctrl	DMSO	10.59 +/- 0.23
	c-Met	22.36 +/- 1.09
	Hh	36.47 +/- 0.85
shRNA-c-Met	DMSO	69.19 +/- 2.56
	c-Met	70.26 +/- 0.98
	Hh	71.17 +/- 1.12

Note: Fisher's test was performed. There is a statistically significant difference ( $p < 0.0001$ ) between the DMSO treated and Hh inhibitor treated KPC tumor cells transfected with shRNA-Ctrl. There is no statistical difference between treatments of cells transfected with c-Met shRNA. Data are shown as the mean +/- standard error of the mean (SEM)

Author Manuscript

Author Manuscript

Author Manuscript

Author Manuscript